

DEFECT IMAGING BY MICROMACHINED ULTRASONIC AIR TRANSDUCERS

Sean Hansen, Neville Irani, F. Levent Degertekin, Igal Ladabaum, and B. T. Khuri-Yakub

Edward L. Ginzton Laboratory
Stanford University
Stanford, CA 94305-4085

Abstract—Capacitive micromachined ultrasonic transducers (cMUTs) are shown to have over 100 dB dynamic range in air. This enables fast imaging of internal defects of solid structures with high signal-to-noise ratio. The high dynamic range is the result of a resonant structure with a fractional bandwidth limited to about 10%. Better temporal resolution is required to differentiate the defects in the depth dimension, which demands higher bandwidth devices.

In this paper we present an optimized pulse-echo electronics system for cMUTs in air. Simulations suggest that dynamic ranges in excess of 100 dB are attainable in pulse-echo operation using commercially available discrete components. Transmission experiments through aluminum and composite plates verify more than 100 dB dynamic range and demonstrate the ability of cMUTs to image defects in air at 2.3 MHz. We also present a variation on cMUT design which improves the useful bandwidth of the device, permitting greater depth resolution in pulse-echo imaging.

INTRODUCTION

Due to the large impedance mismatch between common piezoelectric materials and air, conventional piezoelectric transducers are not very efficient sources of ultrasound in air [1]. While the efficiency can be increased with matching layers, this improvement often comes at the expense of bandwidth. Recently, several capacitive micromachined ultrasonic transducers (cMUTs) have been developed, which are capable of efficient excitation and detection of ultrasound in air [2], [3]. As depicted in Fig. 1, a single element consists of a metalized 0.5-1 μm thick nitride membrane suspended above a silicon substrate. Several thousand such elements are electrically connected in parallel to make the transducer, shown in Fig. 2. When the membranes are biased with a DC bias voltage, the transducer is capable of efficient excitation and detection of ultrasound in air.

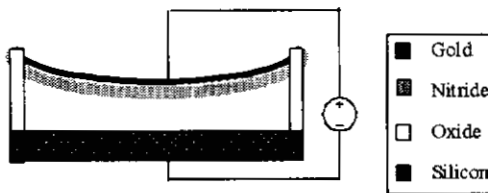


Fig. 1. Schematic cross-section of a single cMUT membrane.

A PULSE-ECHO ELECTRONICS SYSTEM FOR cMUT

The use of cMUTs in monostatic pulse-echo operation requires an electronic system that is capable of handling tone-bursts of tens of volts for the transmitted ultrasound

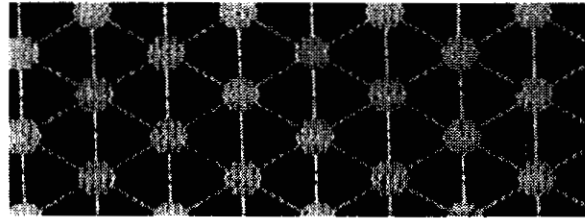


Fig. 2. Magnified view of cMUT transducer with membrane radii of 50 μm .

and amplifying received echos on the order of tens of microvolts. One such electronic system is shown in Fig. 3. In the far left of Fig. 3, the cMUT is modeled as a series RLC circuit in parallel with a capacitor. These elements are sufficient to model the fundamental resonance of the transducer, shown in the impedance curve of Fig. 4. Values for the resistors, inductors, and capacitors are found by curve-fitting data measured from a network analyzer or data from a simulated impedance curve of the transducer for a particular manufacturing process. The resistor of the series RLC is divided into two series resistors. R_{rad} represents the radiation resistance that delivers ultrasound energy into air. The second resistor, R_{loss} , models dissipative losses in the transducer. Simulations and experimental data suggest that the value of the loss resistance is approximately seven times the radiation resistance [4].

Other circuit components include, a coupling capacitor, C_{coup} , which isolates the remaining electronics from the transducer DC bias. A variable inductor, labeled L_{tune} in Fig. 3, cancels the transducer's reactive impedance, resulting in more efficient power delivery to and from the transducer. More complicated matching networks can be implemented to transform the transducer impedance for maximum power delivery. However, following the trans-

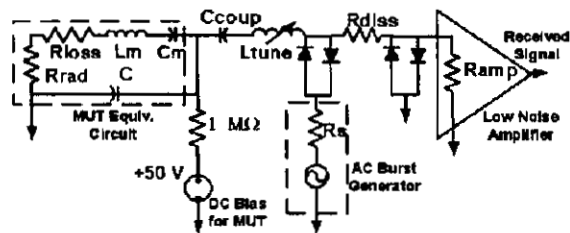


Fig. 3. A pulse-echo electronics system.

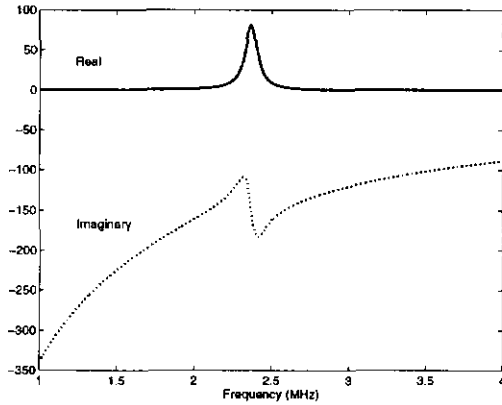


Fig. 4. Real and imaginary impedance of typical cMUT in air.

mit tone-burst, the transducer radiation resistance, R_{rad} , changes its role in the circuit from the load impedance to the source impedance when it receives an echo. Therefore, in general, one cannot provide a matching network that is capable of matching the transducer for maximum power delivery in both the transmit and receive cases. A single tuning inductor is an easily implemented compromise for the system.

The system transmits an ultrasound tone-burst when driven by a large 20 V amplitude AC signal source and some fraction of the available power is dissipated in the radiation resistance as ultrasound in air. The resistor, R_{diss} , in front of the amplifier of Fig. 3 attenuates the AC signal in front of the protection diodes, protecting the amplifier from large voltages at its input. During the transmit tone burst, it is advantageous to use a large value of R_{diss} to minimize the amount of generator power that it shunts away from the transducer.

When the system receives an echo, the AC signal generator is shorted and all of the diodes are effectively off since the received signal amplitude is significantly smaller than the diodes' built-in potentials. The received signal generator can be thought of as an AC voltage source with a source resistance of R_{rad} . Since R_{diss} forms a voltage divider with the input of the amplifier, R_{amp} , it is advantageous to use a small value for R_{diss} for the maximum received signal.

From the preceding discussion, it appears there is an optimum set of values for R_{diss} and R_{amp} which balances the losses during the transmit and receive phases of pulse-echo operation. For a transducer with the impedance curve shown in Fig. 4, the dependence on the received voltage signal at the input of the amplifier for a fixed AC generator voltage is shown in Fig. 5. Typically, the received voltage is more sensitive to the value of R_{diss} than to values of R_{amp} . Since it is not practical to design an amplifier with arbitrary input impedances for use with particular transducers, one may insert a transformer in front of an amplifier that has a known input impedance.

Once values for R_{diss} and the transformer ratio for R_{amp} are selected, complete signal and noise analysis on the full system is possible using SPICE circuit simulation. This

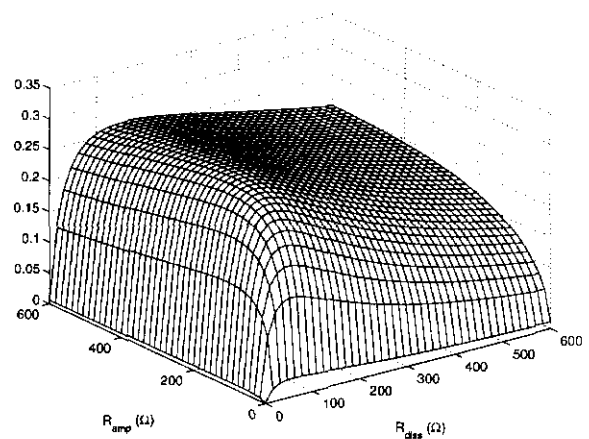


Fig. 5. Variation in received pulse-echo rms voltage signal as a function of R_{diss} and R_{amp} .

analysis accounts for non-ideal signal losses through parasitic capacitances and for all thermal noise sources. The transducer's own thermal noise is accurately represented by R_{rad} and R_{loss} [4]. For the amplifier input, the circuit uses the AD600, a commercially available low-noise amplifier from Analog Devices with an input noise voltage of $1.4 \text{ nV}/\sqrt{\text{Hz}}$. Since the AD600 has an input resistance of 100Ω , a wide range of effective input resistances is available by selecting the appropriate transformer ratio at input to the amplifier. The simulated noise bandwidth is 1 MHz around the transducer resonance, which is easily achieved by filtering the output of the amplifier. Figure 6 shows

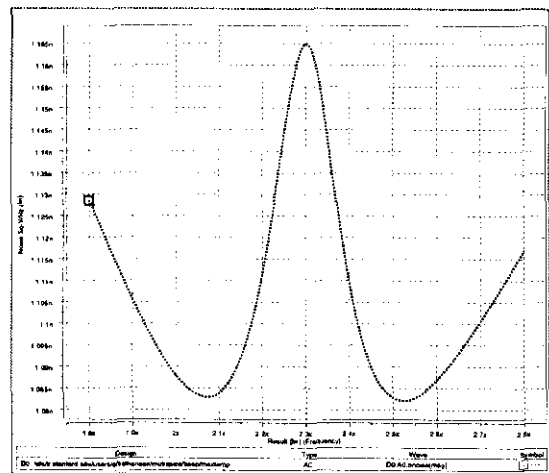


Fig. 6. Noise [V^2/Hz] at amplifier input as a function of frequency.

the squared noise voltage in V^2/Hz at the amplifier input, including a $1.4 \text{ nV}/\sqrt{\text{Hz}}$ noise source in front of the AD600 amplifier. The square-root of the integral of this noise curve yields a noise voltage at the input of the now noiseless amplifier of $1.057 \mu\text{Vrms}$. Since the received echo is 0.216 Vrms when all of the radiated power from R_{rad} is available for reception, the pulse-echo system has a dy-

dynamic range of 106 dB.

A transmission experiment, which uses separate transmit and receive circuits, is capable of a larger dynamic range of operation since it is possible to independently match both the transducer and receiver for maximum available power delivery. Furthermore, there is no need for dissipative elements, such as R_{diss} , or diode protection circuits since the sensitive amplifier is isolated from the transmit signal. When an analysis with the same noise parameters of the preceding example is applied to a transmission experiment, in which both transmitting and receiving circuits are perfectly matched, the simulated dynamic range is 115 dB. These large dynamic ranges, in excess of 100 dB for both pulse-echo and transmission operation, show the applicability of cMUTs for NDE and defect imaging. Further design improvements which reduce the internal loss of the transducer, modeled by R_{loss} , could increase the dynamic range an additional 20-30 dB.

DEFECT IMAGING RESULTS

The simulations of the previous section suggest that the dynamic range of cMUTs is adequate to transmit through materials such as metal and composite plates in air, without the need for coupling fluids. Figure 7 shows the received tone from bistatic transmission through a four-layer carbon fiber composite plate at normal incidence. By varying the amplification of the received signal with and without the sample, we estimate that the composite plate and its interfaces with air attenuate the ultrasound signal by 68 dB. With an additional 6 dB of attenuation due to the air gap at 2.3 MHz, and a 29 dB signal-to-noise ratio, Fig. 7 demonstrates a dynamic range of 103 dB.

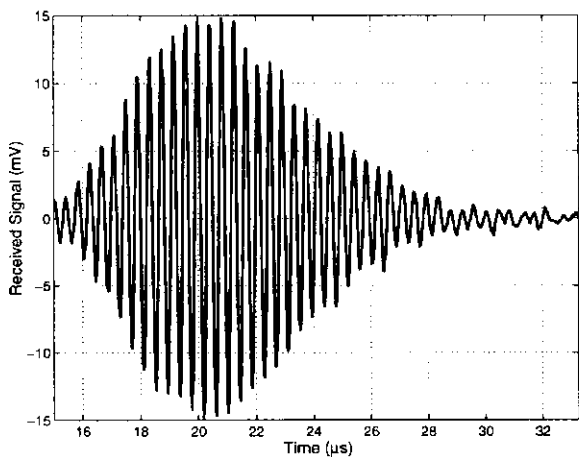


Fig. 7. Received voltage signal through composite plate.

This transmission experiment did not take advantage of any matching networks to boost the power delivery to and from the transducers. Nonetheless, its 29 dB signal to noise ratio, without signal averaging, is adequate to image damage in the composite plate. Figure 8 shows an image produced by linearly gray-scaling the amplitude of the received signal over a section of composite. Density variations in the

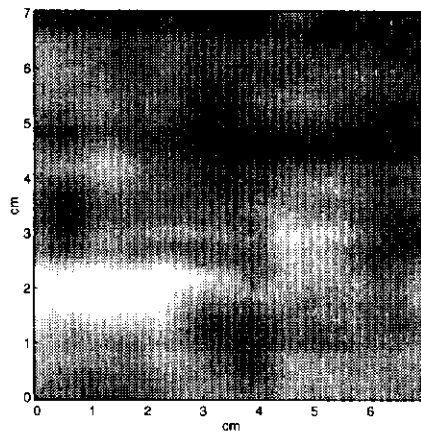


Fig. 8. Amplitude image of composite prior to impact damage.

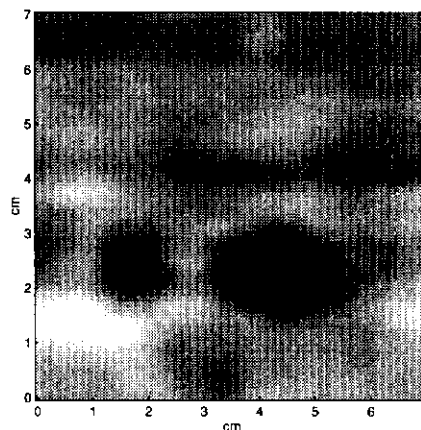


Fig. 9. Amplitude image of composite after impact damage in two places.

plate are evident by regions of light and dark. Figure 9 is produced by scanning the same section of composite plate after the composite was struck in two places, which appear as dark spots in the figure. The leftmost damage spot is not optically visible from the surface, but is clearly present in the ultrasound image.

The image in Fig. 10 shows the amplitude variations in a 3 mm thick aluminum plate that has a 0.5 mm deep pattern milled on the underside of the plate. The dynamic range of the system in this experiment is also about 103 dB, with 82 dB of loss through the aluminum plate at 2.3 MHz.

DYNAMIC FREQUENCY TUNING OF cMUTS

In many ultrasound applications such as pulse-echo imaging, it is desirable to have a wide band transducer to allow shorter excitation tone-bursts. This permits better resolution of reflections in time from varying depths in the material. Although the resonant structure of our current cMUT devices for air results in a large dynamic range, they are inherently narrow band devices with fractional band-

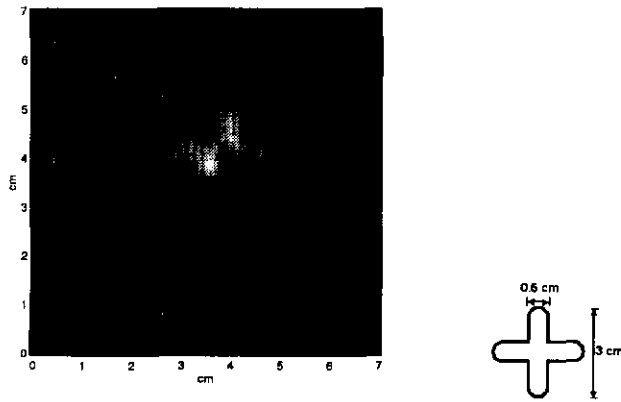


Fig. 10. Amplitude image of milled pattern in aluminum plate.

widths of less than 10%.

In principle, a narrow band transducer can provide the same information as a wide band transducer if it can provide a signal output over the same frequency range. We propose a method by which the resonant frequency of the cMUT can be altered quickly and accurately using piezoelectric actuation. Figure 11 illustrates one method of applying stress which has been tested on an immersion cMUT. Figure 12 shows the shift in a transducer's resonant frequency, as measured on a network analyzer. Computer

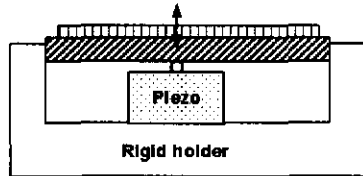


Fig. 11. A possible piezoelectric actuation scheme for dynamic control of cMUT resonance frequency.

simulations on an immersion transducer, shown in Fig. 13, suggest that a wide variation in frequency shifts may be possible with cMUTs. Signals collected from a dynamically strained cMUT in pulse-echo operation can be analyzed in the frequency domain instead of the conventional time domain analysis for a wide band transducer.

CONCLUSION

Electronic circuit simulation suggests that a pulse-echo imaging system using cMUTs is capable of dynamic ranges in excess of 100 dB. Experimental data from transmission experiments demonstrates 103 dB dynamic range without the use of matching networks or signal averaging. This permits defect imaging in aluminum and composite plates. Further development of cMUTs is necessary to improve their ability to temporally resolve defects in a pulse-echo configuration. However, simulations and preliminary experimental results demonstrate the feasibility of dynamically altering the membrane resonance to achieve a wide band response.

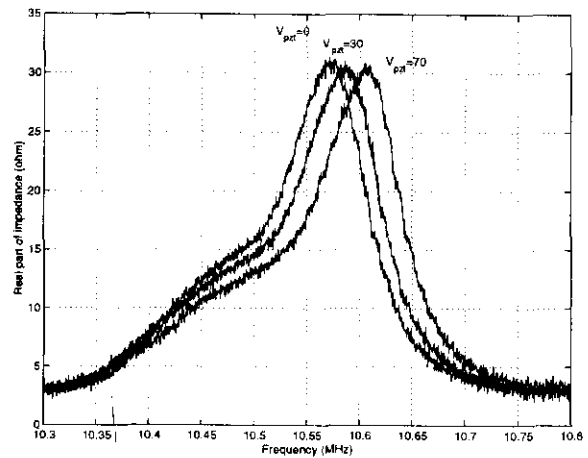


Fig. 12. Experimental test of resonance shift in an immersion cMUT.

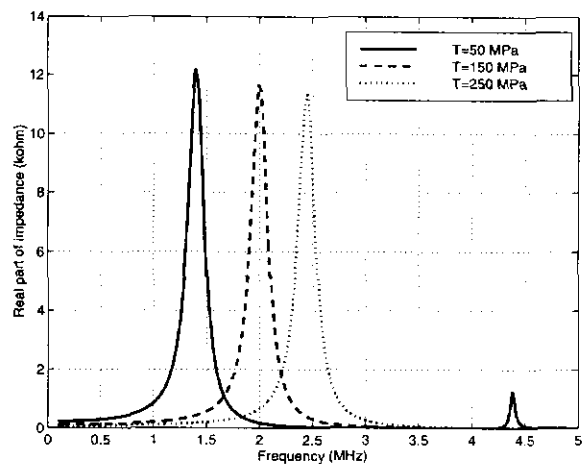


Fig. 13. Simulated resonance shift with changing stress.

ACKNOWLEDGMENTS

This work is supported by WPAFB and the US Office of Naval Research.

REFERENCES

- [1] W.A. Grandia and C.M. Fortunko, "Nde applications of air-coupled ultrasonic transducers," Seattle, WA, November 1995, IEEE Ultrasonics, Ferroelectrics, and Frequency Control Society, pp. 697-709.
- [2] D.W. Schindel and D.A. Hutchins, "Applications of micromachined capacitance transducers in air-coupled ultrasonics and nondestructive evaluation," *IEEE Trans. on Ultrasonics, Ferroelectrics and Frequency Control*, vol. 42, no. 1, pp. 51-8, January 1995.
- [3] M. I. Haller and B. T. Khuri-Yakub, "A surface micromachined electrostatic ultrasonic air transducer," *IEEE Trans. on Ultrasonics, Ferroelectrics and Frequency Control*, vol. 43, no. 1, pp. 1-6, January 1996.
- [4] I. Ladabaum, X. C. Jin, H. T. Soh, A. Atalar, and B. T. Khuri-Yakub, "Surface micromachined capacitive ultrasonic transducers," *IEEE Trans. on Ultrasonics, Ferroelectrics and Frequency Control*, vol. 45, no. 3, pp. 678-690, May 1998.